ELSEVIER

Journal of Alloys and Compounds 320 (2001) 114–125

Journal of ALLOYS AND COMPOUNDS

www.elsevier.com/locate/jallcom

Thermally stimulated solid state reactions in Fe–Al multilayers prepared by pulsed laser deposition

A.A. Levin[a], D.C. Meyer[a], P. Paufler[a,*], A. Gorbunov[b], A. Tselev[b], P. Gawlitza[c]

[a]*Institut für Kristallographie und Festkörperphysik, Fakultät Mathematik und Naturwissenschaften, Technische Universität Dresden, D-01062 Dresden, Germany*

[b]*Institut für Werkstoffwissenschaft, Fakultät Maschinenwesen, Technische Universität Dresden, D-01062 Dresden, Germany*

[c]*Fraunhofer-Institut für Werkstoff- und Strahltechnik, D-01277 Dresden, Germany*

Received 18 January 2001; accepted 26 January 2001

Abstract

Two 15-period Fe–Al multilayers (single layer thicknesses ~5 nm Al and ~2 nm Fe) prepared by direct and crossed-beam pulsed laser deposition (DPLD and CBPLD, respectively) were subjected to annealing between 50 and 950°C. Phase analysis done by X-ray diffraction and determination of layer morphology using X-ray reflectometry showed that solid state reaction kinetics is different in DPLD and CBPLD samples. This applies in particular to the sequence of intermetallic compounds formed as well as to the temperatures of full intermixing. Pronounced interdiffusion of Fe and Al starts at annealing temperatures of about 110 –140°C and a full intermixing of multilayer material occurs at temperatures between 250°C (DPLD) and 300°C (CBPLD). The difference in kinetics between CBPLD and DPLD samples is due to a difference in the structure of interfaces and in their average chemical composition. © 2001 Elsevier Science B.V. All rights reserved.

Keywords: Laser ablation; Thin films; X-ray diffraction; Reaction kinetics

1. Introduction

Fe–Al multilayers (MLs) with film thickness on nanometer scale have received considerable attention in recent years mostly because of interesting magnetic and mechanical properties [1–6]. It is known from the equilibrium phase diagram [7] that a high solubility of Al (up to 20 at.% at room temperature) exists in α-Fe (W type of structure, space group $Im\bar{3}m$, $a = 0.28665$ nm [8]) whereas α-Fe is practically insoluble (up to 0.04 at.% at room temperature) in Al (Cu type, space group $Fm\bar{3}m$, $a = 0.40488$ nm [8]).

Knowing the mechanism of pulsed laser deposition (PLD), two different kinds of interfaces can be expected in Fe–Al MLs, i.e. the interface formed by deposition of Fe onto an Al layer (Fe-on-Al) and that caused by deposition of Al onto an Fe layer (Al-on-Fe). While as-deposited Fe–Al MLs prepared by other methods such as thermal evaporation [9], magnetron sputtering [5] and molecular beam epitaxy [10] show rather sharp interfaces, those prepared by PLD techniques have rather thick transition regions between adjacent layers [9,11–15]. That is because PLD is characterised by a relatively large mean kinetic energy of deposition plasma particles ranging from typically 100 eV in crossed-beam pulsed laser deposition (CBPLD) [16] to 200–300 eV in conventional direct PLD (DPLD) [17]. As a consequence, condensation of layer material during deposition proceeds far from thermodynamic equilibrium, thus enabling enhanced solid solubility and non-conventional phase formation to occur. One goal of CBPLD is to avoid contaminations of films with microsized particles (droplets, debris), which very often occur with DPLD samples.

Phase formation in Fe–Al MLs under thermal treatments has been investigated by several authors [5,18,19]. Solid state reactions of Fe–Al_2O_3 MLs deposited by magnetron sputtering have been studied in Ref. [5]. A single phase α-Fe was observed up to an annealing temperature of about 700°C. Above this temperature the α-Fe phase was in coexistence with other equilibrium phases as γ-Fe, FeAl and $FeAl_2O_4$. Interaction between couples of solid Fe and liquid Al have been investigated in Ref. [18].

Recently, authors of the present paper have studied the

*Corresponding author.

E-mail address: paufler@physik.phy.tu-dresden.de (P. Paufler).

0925-8388/01/$ – see front matter © 2001 Elsevier Science B.V. All rights reserved.
PII: S0925-8388(01)00941-0

structural modifications of certain CBPLD prepared Fe–Al Mls (samples CBPLD1) with nominal composition 5*(5 nm Fe–5 nm Al) by annealing at temperatures ranging between 100 and 300°C [19]. It was found that pronounced interdiffusion of Fe and Al starts at an annealing temperature of about 150°C preferably at the Fe-on-Al interfaces. The formation of the intermetallic phase FeAl was observed at the same temperature. This compound comprised the entire multilayer (apart from top layers of Al and Al_2O_3) after annealing above 250°C.

The aim of the present paper is to report on an extension of both the annealing temperatures from 300 to 950°C and the number of double layers from 5 to 15 for MLs characterized by a lower thickness of Fe layers ($t_{Fe}=2$ nm) as well as on a comparison of the reaction kinetics between Fe–Al MLs prepared by the different methods — CBPLD and conventional DPLD.

2. Experimental

Fe–Al MLs with similar compositions were prepared by CBPLD and conventional DPLD. A multilayer with a total nominal stack thickness of about 110 nm and a nominal composition 15*(5 nm Al–2 nm Fe)–5 nm Al deposited on oxidised silicon wafer (thickness of the oxide layer is about 500 nm) was prepared by CBPLD according to Ref. [20].

Another multilayer with nominal composition 5 nm Al–15*(5 nm Al–2 nm Fe)–2 nm Al and a total nominal stack thickness of about 112 nm was deposited by conventional DPLD. Details of preparation are given in Ref. [14]. A silicon wafer covered with natural silicon oxide (thickness about 2.5 nm) was used.

Samples were annealed step by step in a tubular furnace in vacuum under $<10^{-5}$ mbar at temperatures ranging between 50 and 950°C. The duration of every single step of annealing was approximately 15 min. Before and after each step of annealing, the structure of the MLs was checked by means of X-ray reflectometry and wide-angle X-ray scattering (WAXS). Then annealing was continued for another 15 min at the same temperature if reflection curves or X-ray diffraction patterns of samples showed significant changes. After stabilisation of the structure of MLs at a certain temperature, a higher annealing temperature was applied.

The crystal phase composition of MLs was analysed by means of WAXS using an X-ray diffractometer URD-6 (Seifert FPM) with CuKα graphite-monochromatised radiation. As reflections in $\theta/2\theta$ scan mode come only from net planes parallel to the sample surface, single θ and 2θ scan modes were also used to reveal reflections hidden by texture. Thereby either 2θ or θ was fixed.

Reflection curves were recorded in $\theta/2\theta$ specular scan mode using an X-ray diffractometer (HZG-4, Seifert FPM) with a Si(111) monochromator tuned to the Kβ-energy of a tube with Cu anode. The parameters of the layers (thickness and densities of layers and roughness of interfaces) were determined by fitting the curves to experimental the reflectograms exhibiting Bragg superlattice peaks and Kiessig fringes. Refinement of parameters was done using the computer program REFSIM (S. Grassl, D. Fuchs et al., Siemens AG, 1994), which relies on the recursive approach for MLs of Parrat [21].

3. Results and discussion

3.1. X-ray reflectometry

Experimentally determined reflection curves for some characteristic temperatures of annealing are shown together with best fit model curves (dashes) in Fig. 1.

A summary of the best fit of our experimental results is schematically presented in Fig. 2 (see also Tables 1 and 2). The thickness of structure blocks drawn by solid lines and the roughness of interfaces shown by hatched regions were put on an absolute scale for each sample. The best fits to the experimental reflection curves of the DPLD sample at different annealing stages could be obtained using two structure blocks instead of one nominal period. The same grouping of layers in two blocks is used for both the DPLD and the CBPLD samples for an easier comparison of the structures. Each stacking model is valid only in a limited temperature range. The temperatures, at which the structure of the MLs significantly changes, are indicated at the bottom of Fig. 2.

According to [9,11–15], the formation of Fe–Al transition layers (TLs) between adjacent Fe and Al layers is assumed to occur due to intermixing of Fe and Al atoms at the interfaces during deposition by PLD techniques. As this assumption was based on results of Mössbauer spectroscopy, X-ray absorption fine structure and transmission electron microscopy experiments, we have introduced these TLs into the structure model of as-prepared MLs (Fig. 2, stage 1) instead of the usual model of nominal Fe–Al stacking. The average composition of TLs was estimated to be $Fe_{44}Al_{56}$ for the CBPLD samples and $Fe_{40}Al_{60}$ for the DPLD samples considering the different atomic densities of as-deposited layers according to the procedure described in [19]. This modified model gave a much better fit of the experimental reflection curves and a significant decrease of the remaining interface roughness parameters [22].

As can be seen from Fig. 2, the Al layers first start to dissolve during annealing. The TLs become thicker after thermal treatment at rather low temperature of about 110°C. After annealing at temperatures of about 140°C, no Al-rich layers (apart from the top thick Al layer) were observed in CBPLD multilayers. The multilayer period consisted only of Fe and Fe–Al layers (stage 2, CBPLD sample, Fig. 2a). At the same temperature, in the DPLD

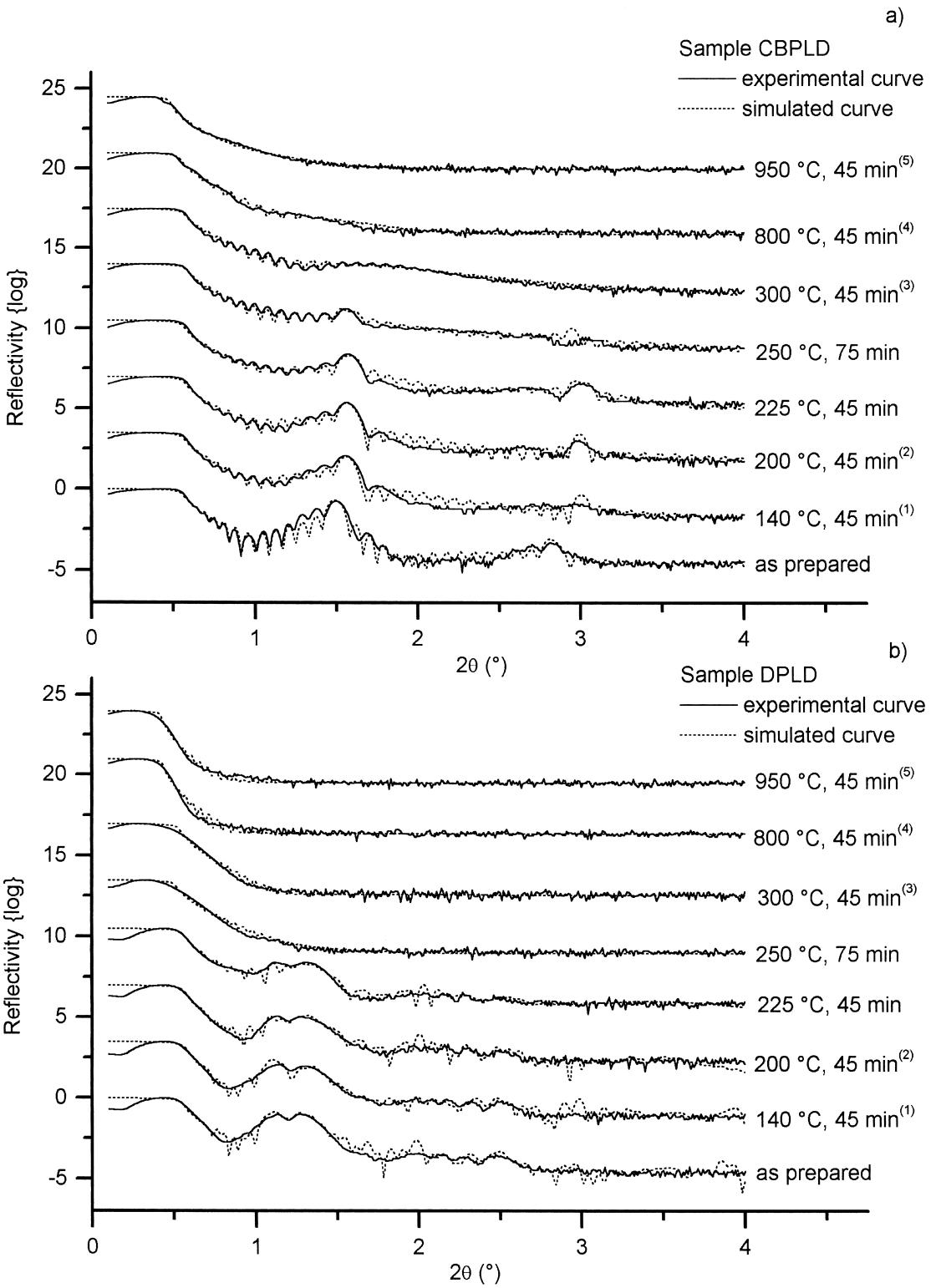

Fig. 1. Measured (solid lines) and calculated (dashed) reflectivity versus diffraction angle for the CBPLD (a) and DPLD (b) samples. Reflection curves after each annealing step were shifted for better visual perception. Simulated curves for the CBPLD sample were calculated using model 1 for the as-prepared multilayer and the state at 50–110°C, model 2 for 140–275°C, model 3 for 300–750°C and model 4 for 800–950°C. Simulated curves for DPLD sample were calculated using model 1 for the as-prepared multilayer and the state at 50–110°C, model 2 for 140–170°C, model 3 for 200–225°C, model 4 for 250–750°C, and model 5 for 800–950°C. Sample geometry corresponding to these models is shown in Fig. 2. The model number corresponds to the stage number in Fig. 2 and Tables 1 and 2. (1) 50°C, 45 min + 80°C, 60 min + 110°C, 60 min + 140°C, 45 min; (2) 170°C, 45 min + 200°C, 45 min; (3) 275°C, 45 min + 300°C, 45 min; (4) 330°C, 60 min + 350°C, 45 min + 375°C, 45 min + 410°C, 45 min + 440°C, 45 min + 470°C, 45 min + 500°C, 45 min + 530°C, 45 min + 565°C, 45 min + 600°C, 60 min + 650°C, 45 min + 675°C, 45 min + 700°C, 45 min + 750°C, 45 min + 800°C, 45 min; (5) 825°C, 45 min + 850°C, 45 min + 900°C, 45 min + 950°C, 45 min.

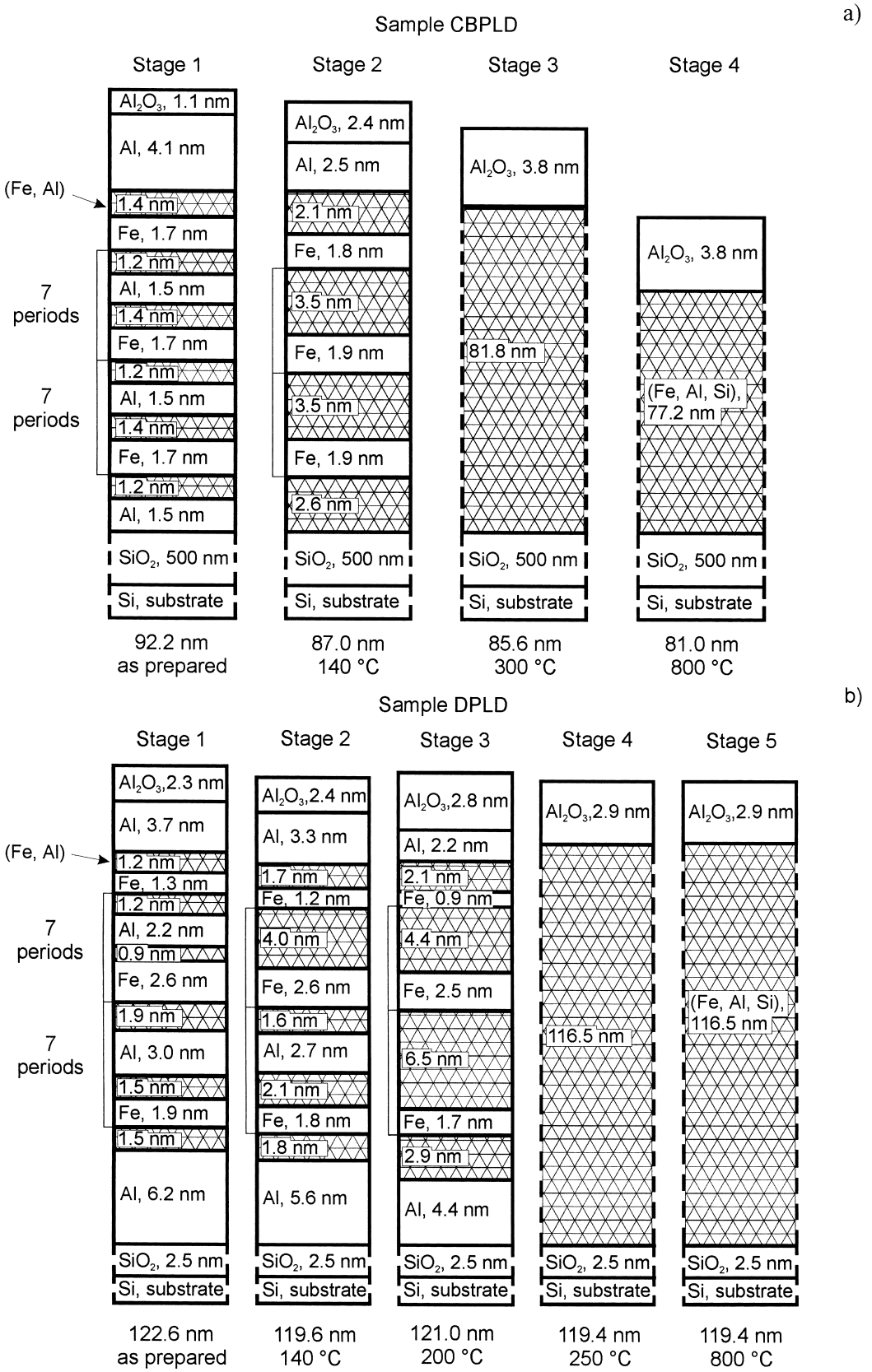

Fig. 2. Scheme of CBPLD (a) and DPLD (b) sample geometry for successive stages of annealing. The experimental layer thickness is indicated. Total thickness of the film and the lower boundaries of the temperature intervals where each model yielded a satisfactory fit are indicated at the bottom. Layers with average composition are marked as (Fe, Al). Average composition is $Fe_{44}Al_{56}$ and $Fe_{40}Al_{60}$ for samples CBPLD and DPLD, respectively. Layers with incorporation of Si at last stages of annealing are marked as (Fe, Al, Si). Estimated average compositions of the layers are $Fe_{21}Al_{27}Si_{52}$ and $Fe_{14}Al_{22}Si_{64}$ for samples CBPLD and DPLD, respectively.

sample the Al-rich layers were completely dissolved in one of the structural blocks (stage 2, sample DPLD, Fig. 2b).

Dissolution of Al in the second structural block of the DPLD sample was detected after thermal treatment at a temperature of about 200°C. Only relatively thick top and bottom Al layers are preserved in the structure at this annealing temperature (stage 3, sample DPLD, Fig. 2b). The same phenomenon of dissolution of Al layers at one of the first stages of annealing in the same temperature range has been observed recently during the thermal treatments of comparable 5-period Fe–Al MLs [19]. Probably, this non-simultaneous disappearance of Al layers is due to different thicknesses of the layers.

Annealing at higher temperatures results in full intermixing of multilayer material (apart from top cover alumina layer) at temperatures of about 250 and 300°C for DPLD and CBPLD samples, respectively. The films then consist of thick monolayers with average Fe–Al composition covered by alumina layer (stage 3 of sample CBPLD and stage 4 of sample DPLD, Fig. 2). Whereas at lower temperature of about 250°C [19] full intermixing of multilayer material was observed in 5-period CBPLD1 samples (total nominal thickness of about 50 nm), this was not the case in 15-period CBPLD multilayers with total nominal thickness of about 110 nm.

When calculating the average Al content of the samples in the various stages of thermal treatment according to $X_{Al} = [\Sigma t \cdot x_{Al}]/[\Sigma\ t]$ a change was found. In this expression, t are the layer thicknesses and x_{Al} are the Al contents of layers (in at.%) estimated on base of experimental layer densities from Tables 1 and 2 (knowing the bulk densities of crystalline Al and Fe). In the CBPLD sample, X_{Al} decreased from 62(8) at.% in the as-prepared state to 57(8) at.% in the stage of full intermixing ($T = 300$°C). A similar tendency was observed after thermal treatment of 5-period Fe–Al MLs [19] prepared by CBPLD: X_{Al} decreased from 47(8) at.% in as-prepared MLs to 35–39(8) at.% in samples after final annealing ($T = 300$°C). Contrary to the CBPLD sample, the average Al content X_{Al} of DPLD sample shifted from 64(8) at.% in as-prepared multilayer to higher values of about 75(8) at.% in the state of full intermixing ($T = 250$°C). As the nominal compositions of DPLD and CBPLD samples were close to each other, the difference in actual average compositions should be due to the method of layer deposition.

With annealing at 800°C, samples changed their colour from a steel shade to mat dark-yellow (DPLD) or dark-violet (CBPLD specimen). This was found to be accompanied by a sharp decrease of the density of the remaining thick monolayer to 3.6 $g \cdot cm^{-3}$ for the CBPLD and to 3.2 $g \cdot cm^{-3}$ for the DPLD sample. It is reasonable to conclude that Si started to be incorporated into the film. Using these experimental densities, the average composition of the monolayers was estimated to be $Fe_{21}Al_{27}Si_{52}$for CBPLD and $Fe_{14}Al_{22}Si_{64}$ for DPLD specimen assuming the same Fe:Al ratio as at the previous stages of annealing (stage 4 of sample CBPLD and stage 5 of sample DPLD, Fig. 2).

Table 1
Parameters of individual layers (thickness t, roughness σ, density ρ) of the CBPLD multilayer determined by fitting the models to the experimental reflection curves. Numbers of stages are given according to Fig. 2a. Standard deviations of thickness, roughness and density are about of 0.4 nm, 0.3 nm and 0.3 g/cm^3, respectively

Layer	Sample CBPLD		
	t (nm)	σ (nm)	ρ (g/cm^3)
Stage 1, as prepared			
Al_2O_3	1.1	0.1	2.5
Al	4.1	0.1	2.6
$Fe_{44}Al_{56}$ [a,p]	1.4	0.3	4.5
Fe[p]	1.7	0.1	6.6
$Fe_{44}Al_{56}$[a,p]	1.2	0.3	4.4
Al[p]	1.5	0.1	3.0
SiO_2	500[f]	0.3	2.5
Stage 2, 140°C			
Al_2O_3	2.4	1.1	2.5
Al	2.5	0.2	2.6
$Fe_{44}Al_{56}$[a]	2.1	0.2	5.2
Fe	1.8	0.6	5.5
$Fe_{44}Al_{56}$[a,p]	3.5	0.9	4.1
Fe[p]	1.9	1.0	6.4
$Fe_{44}Al_{56}$[a]	2.6	0.7	4.7
SiO_2	500[f]	1.1	2.6
Stage 3, 300°C			
Al_2O_3	3.8	1.1	2.2
$Fe_{44}Al_{56}$[a]	81.8	0.3	4.9
SiO_2	500[f]	1.5	2.6
Stage 4, 800°C			
Al_2O_3	3.8	2.0	1.9
$Fe_{21}Al_{27}Si_{52}$[a]	77.2	1.2	3.8
SiO_2	500[f]	4.3	2.5

[a] Average composition.
[p] Layer in period (Stage 1: 15 periods; Stage 2: 14 periods).
[f] Fixed value.

3.2. Wide-angle X-ray diffraction

Diffraction patterns for some characteristic annealing temperatures recorded in $\theta/2\theta$ scan mode are shown in Figs. 3 and 4 for CBPLD and DPLD samples, respectively. Also 2θ scans (θ is fixed at 21.50°) were carried out for both the samples. The strongest peaks of the diffraction patterns in Figs. 3 and 4 are the substrate peaks from single-crystalline (001) Si wafers.

Because of a strong fibre texture, the diffraction patterns of as-prepared MLs have only a small number of non-substrate reflections.

Similarly to CBPLD1 MLs [19], only one non-substrate reflection is present in the diffraction pattern of the as-prepared CBPLD sample. The diffraction pattern of an as-prepared DPLD multilayer showed four non-substrate reflections. One of them is similar to that of the CBPLD multilayer (the corresponding interplanar spacing d_{hkl} is about 0.209 nm) and is attributed to an α-Fe structure type solid solution of Fe and Al (110 Fe reflection in Figs. 3 and 4). Additional three non-substrate reflections have

Table 2
Parameters of individual layers (thickness t, roughness σ, density ρ) of the DPLD multilayer determined by fitting the models to the experimental reflection curves. Numbers of stages are given according to Fig. 2b. Standard deviations of thickness, roughness and density are about of 0.4 nm, 0.3 nm and 0.3 g/cm^3, respectively

Layer	Sample DPLD		
	t (nm)	σ (nm)	ρ (g/cm^3)
Stage 1, as prepared			
Al_2O_3	2.3	0.2	1.9
Al	3.7	0.1	2.7
$Fe_{40}Al^{a}_{60}$	1.2	0.3	4.7
Fe	1.3	0.3	6.6
$Fe_{40}Al^{a,p}_{60}$ (1)	1.2	0.2	5.3
Al^{p} (1)	2.2	0.8	2.8
$Fe_{40}Al^{a,p}_{60}$ (1)	0.9	0.5	4.3
Fe^{p} (1)	2.6	0.6	6.0
$Fe_{40}Al^{a,p}_{60}$ (2)	1.9	0.5	5.0
Al^{p} (2)	3.0	0.6	2.7
$Fe_{40}Al^{a,p}_{60}$ (2)	1.5	0.5	5.5
Fe^{p} (2)	1.9	0.4	7.2
$Fe_{40}Al^{a}_{60}$	1.5	0.7	4.3
Al	6.2	0.5	2.7
SiO_2	2.5[f]	0.6	2.3
Stage 2, 140°C			
Al_2O_3	2.4	0.4	1.9
Al	3.3	0.6	3.1
$Fe_{40}Al^{a}_{60}$	1.7	0.8	3.9
Fe	1.2	0.1	6.6
$Fe_{40}Al^{a,p}_{60}$ (1)	4.0	0.9	4.3
Fe^{p}(1)	2.6	0.5	6.1
$Fe_{40}Al^{a,p}_{60}$ (2)	1.6	0.2	4.4
Al^{p} (2)	2.7	0.5	2.7
$Fe_{40}Al^{a,p}_{60}$ (2)	2.1	0.7	5.1
Fe^{p} (2)	1.8	1.0	6.1
$Fe_{40}Al^{a}_{60}$	1.8	0.7	4.0
Al	5.6	0.4	3.0
SiO_2	2.5[f]	0.4	2.4
Stage 3, 200°C			
Al_2O_3	2.8	0.1	2.3
Al	2.2	0.2	2.9
$Fe_{40}Al^{a}_{60}$	2.1	0.5	4.3
Fe	0.9	0.4	5.4
$Fe_{40}Al^{a,p}_{60}$ (1)	4.4	0.9	4.2
Fe^{p} (1)	2.5	0.8	5.6
$Fe_{40}Al^{a,p}_{60}$ (2)	6.5	0.9	4.0
Fe^{p} (2)	1.7	1.2	5.8
$Fe_{40}Al^{a}_{60}$	2.9	0.8	4.0
Al	4.4	0.7	2.9
SiO_2	2.5[f]	0.9	2.4
Stage 4, 250°C			
Al_2O_3	2.9[f]	1.2	2.0
$Fe_{40}Al^{a}_{60}$	116.5[f]	2.1	4.0
SiO_2	2.5[f]	2.0	2.5
Stage 5, 800°C			
Al_2O_3	2.9[f]	2.8	1.0
$Fe_{14}Al_{22}Si^{a}_{64}$	116.5[f]	4.8	2.8
SiO_2	2.5[f]	1.9	2.4

[a] Average composition.
[p] Layer in period (p1: 7 periods; p2: 7 periods).
[f] Fixed value: disappearance of oscillations in reflection curves (presumably due to 'smearing-out' of Al droplets) did not allow to determine the thickness of the monolayer for stages 4–5. We fitted the reflection curves by fixing the thickness of the layer to the value determined in previous stages of annealing.

sharper shape and are most probably attributed to pure Al due to Al droplets on the surface [12].

Apparently, the Al-rich layers having the thickness of about 5 nm are amorphous in the CBPLD case and probably in the DPLD sample, too, in accordance with data of Refs. [11–13,19] for Fe–Al MLs with thickness of Al layers less than 6 nm.

Figs. 3 and 4 reveal changes of the phase composition due to annealing. In Fig. 5 we have plotted relevant parameters versus annealing temperature for all non-substrate reflections existing in as-prepared samples along with the new reflections arising after annealing. To facilitate the analysis of the occurring reactions, Miller indices of the new reflections (also, those hidden by the texture) are indicated at the corresponding temperatures.

The reflection observed for the as-prepared CBPLD multilayer (110 Fe in Fig. 3) shifts noticeably to higher values of diffraction angle 2θ during annealing in the temperature range of about 50–110°C (Figs. 3 and 5a). The shift continues slowly after annealing in the temperature range 140–750°C and then jumps quickly after thermal treatments at 750–850°C. Annealing at higher temperatures resulted again in a slow decrease of the corresponding interplanar spacings. At the same time, the full width at half maximum (FWHM) of this reflection decreased slowly in the temperature range 50–225°C and then quickly in the temperature range of about 225–330°C. Further treatments did not influence the FWHM value which remained practically constant (Fig. 5a). Maximum and integrated intensities of the reflection increased slowly after annealing at temperatures of about 50–225°C. A considerable increase of the intensities started after 250°C thermal treatment and then stopped at a temperature of about 470°C. Finally, intensities decreased after annealing at temperatures higher than 850°C. Possible alterations of the phases with temperature are shown at the bottom of Fig. 5.Within the temperature range 50–300°C the data of Fig. 5a agree well with those recently observed for the five-period CBPLD1 MLs in [19].

A summary of the temperature ranges where different crystal phases have been observed is shown in Fig. 6 for both the CBPLD and DPLD samples.

It seems worthwhile looking at the formation of the compound FeAl (CsCl type, space group $Pm\bar{3}m$, a = 0.2909 nm [8]), which is a dominating phase in the equilibrium phase diagram [7]. It was found to form at 150°C in 5-period Fe–Al MLs prepared by CBPLD [19]. The average composition of these specimens was estimated as $Fe_{60}Al_{40}$. Probably, an Fe:Al ratio close to 1 ($Fe_{44}Al_{56}$ for CBPLD sample) or larger than 1 promotes the formation of this compound. An Al-rich composition ($Fe_{40}Al_{60}$ for DPLD specimen) apparently prevents this phase from being formed during the first stages of annealing. These observations agree with the equilibrium phase diagram data [7]. According to that FeAl should form at an Al content of approximately 23.3 –55 at.%. From our present data we conclude that FeAl most probably started to form

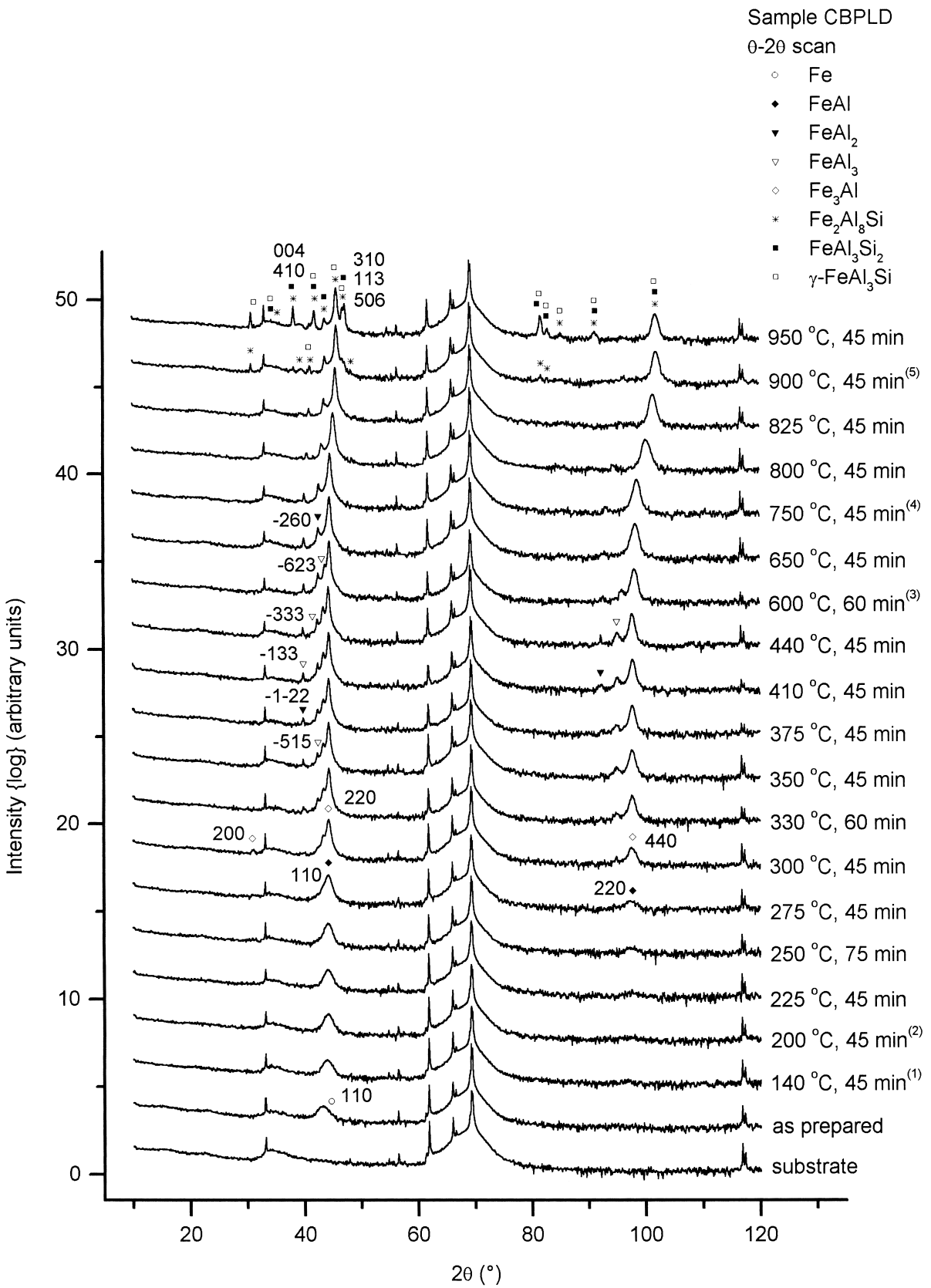

Fig. 3. Intensity versus diffraction angle (θ–2θ scan) for the CBPLD Fe–Al sample after thermal treatments. Diffraction patterns measured after successive steps of annealing were shifted for better visual investigation. Diffraction pattern of the substrate is given for comparison. Theoretical positions of reflections of crystalline phases are shown by marks indicated in the upper right part of the figure. Miller indices of only some reflections are shown for easy visual perception. (1) 50°C, 45 min + 80°C, 60 min + 110°C, 60 min + 140°C, 45 min; (2) 170°C, 45 min + 200°C, 45 min; (3) 470°C, 45 min + 500°C, 45 min + 530°C, 45 min + 565°C, 45 min + 600°C, 60 min; (4) 675°C, 45 min + 700°C, 45 min + 750°C, 45 min; (5) 850°C, 45 min + 900°C, 45 min.

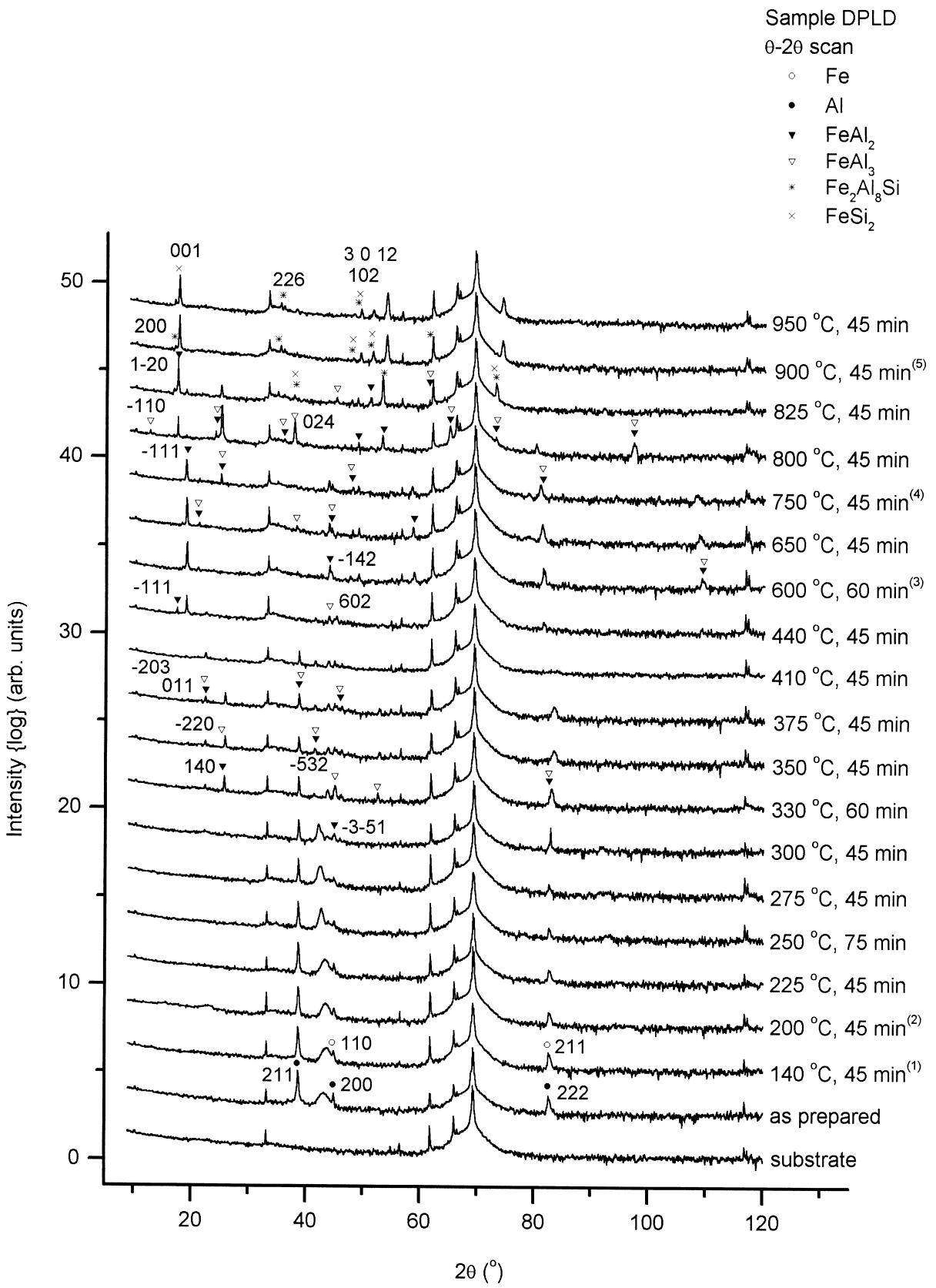

Fig. 4. Same as Fig. 3 for the DPLD sample.

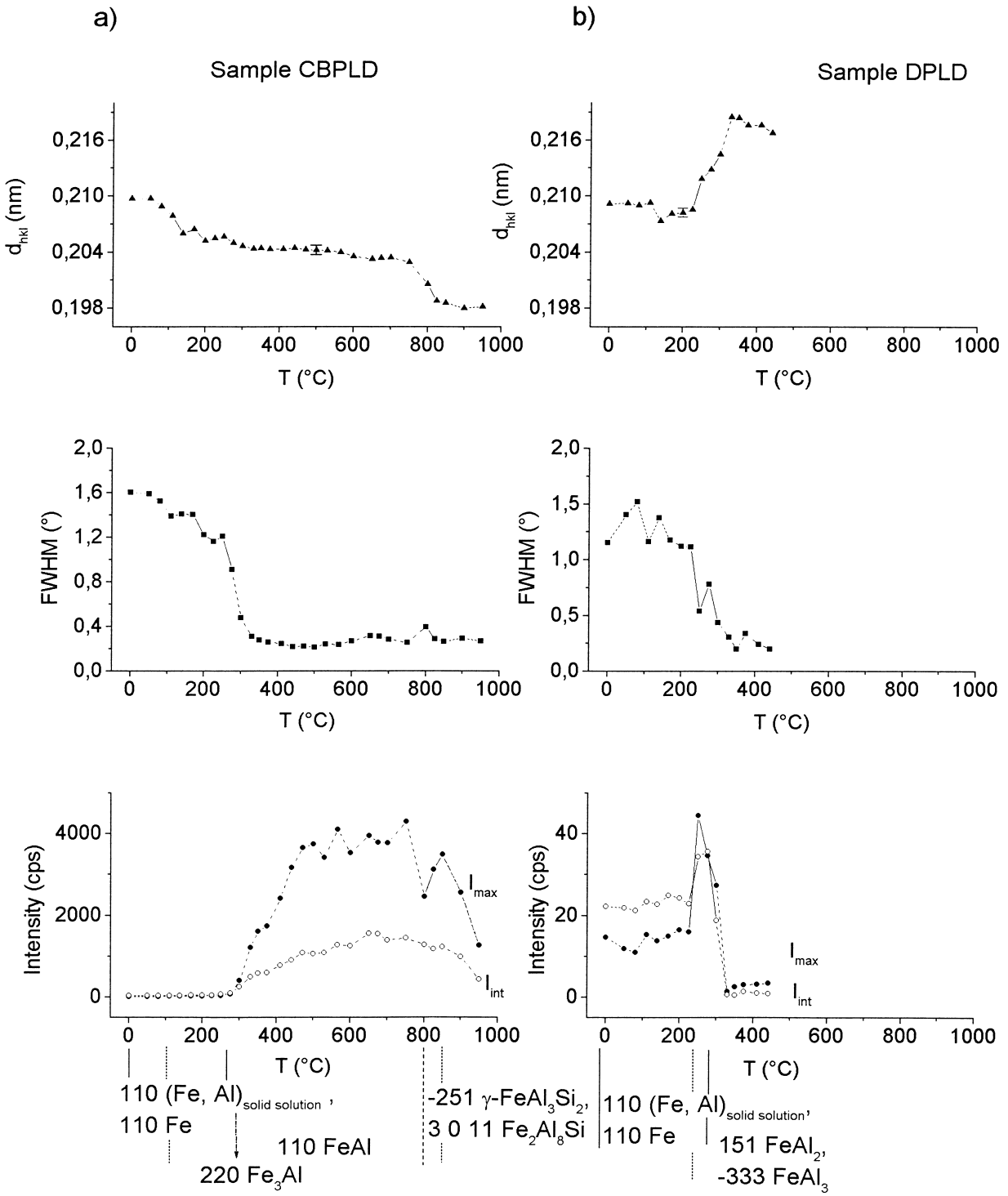

Fig. 5. Interplanar spacing d_{hkl}, FWHM, maximum (I_{max}) and integral (I_{int}) intensities of a reflection characterized by $d_{hkl} \approx 0.209$ nm in the as-prepared state versus annealing temperature for the CBPLD (a) and the DPLD (b) sample. Lines are given as a guide for the eyes. Miller indices of reflections forming after annealing are shown at the bottom. Estimated temperature ranges are indicated in which corresponding phases are observed.

in the CBPLD multilayer at about 110°C (Figs. 3 and 6a). After thermal treatment at 850°C, this phase seemed to disappear again.

Thus, the thermal behaviour of the present 15-period CBPLD multilayer and 5-period CBPLD1 samples [19] is similar up to 250°C. α-Fe-like Fe–Al solid solution crystal

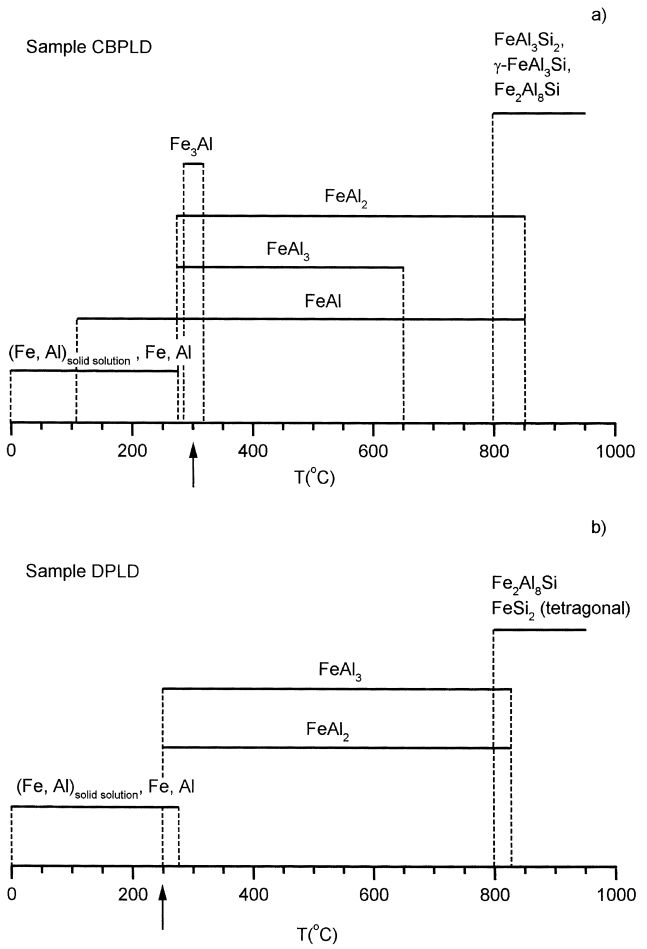

Fig. 6. Ranges of annealing temperatures in which crystalline phases are observed for CBPLD (a) and DPLD (b) samples. High-temperature phases Fe_2Al_8Si and $FeAl_3Si_2$ may also be designated alternatively (see text). Arrows indicate the temperatures of complete intermixing of Fe–Al multilayers.

phase is found in the as-prepared samples. FeAl intermetallic starts to form after annealing at temperature of about 110°C (CBPLD) and 150°C (CBPLD1).

Only this intermetallic phase was detected in CBPLD1 samples after thermal treatments at temperatures up to 300°C [19]. Contrary to CBPLD1 MLs, new reflections in the CBPLD sample start to form at about 275°C (Figs. 3, 6a). The reflections are attributed to the formation of other compounds: $FeAl_3$ (space group *C2/m*, $a=1.5489$ nm, $b=0.80831$ nm, $c=1.2476$ nm, $\beta=107.72°$ [8]) and $FeAl_2$ (space group *P1*, $a=0.7594$ nm, $b=1.6886$ nm, $c=0.4863$ nm, $\alpha=89.55°$, $\beta=122.62°$, $\gamma=90.42°$ [8]). Reflections of the $FeAl_3$ phase disappear after treatment at a temperature of about 650°C.The $FeAl_2$ phase reflections vanish approximately at the same temperature, when the FeAl compound disappears (850°C).

The phase Fe_3Al (BiF_3 type, space group $Fm\bar{3}m$, $a=$ 0.5792 nm [8]) was observed in the CBPLD multilayer in a limited temperature range around 300°C (see Fig. 3). After annealing of the CBPLD sample at 800°C, a reaction between the Si wafer and the Fe–Al multilayer started, resulting in the formation of aluminium iron silicides: Fe_2Al_8Si [1] (*P6₃/mmc*, $a=1.24056$ nm, $c=2.6236$ nm [8,24]), $FeAl_3Si_2$ [2] (Ga_5Pd type, *I4/mcm*, $a=0.607$ nm, $c=0.950$ nm [8]) and γ-$FeAl_3Si$ (P* [3], $a=1.78$ nm, $b=$ 1.025 nm, $c=0.890$ nm, $\beta=132.00°$ [26]). The sample changed its colour from brilliant-steel shade to mat dark-violet (illumination with visible light, inspection by naked eyes). Apparently, the phenomenon gives an additional evidence that aluminium iron silicides were formed after annealing at 800°C.

The solid state reaction processes of the DPLD sample are more complex and quite different. Contrary to the corresponding reflection of the CBPLD sample, d_{hkl} of the broad non-substrate reflection (110 Fe in Fig. 4) is practically constant between 50 and 225°C (Fig. 5b). Then d_{hkl} increased after annealing at 250–330°C, while it decreased slightly in the range 350–440°C (the reflection disappeared at higher temperatures). These changes of d_{hkl}were accompanied by a slow decrease of the FWHM. Changes of the reflection intensities are considerably smaller than those observed for the CBPLD multilayer (see Fig. 5). This behaviour agrees again with the formation of $FeAl_2$ and $FeAl_3$, which started at about 250°C (Figs. 4 and 6b). These phases seemed to be present in the DPLD sample in an extended range of annealing temperatures up to approximately 825°C. One can identify two stages of recrystallisation of these phases at about 440 and 800°C with the aid of reflections appearing after recrystallisation.

The fact that intermixing of the multilayer was accompanied by the formation of $FeAl_2$ and $FeAl_3$ in DPLD and of FeAl, $FeAl_2$, $FeAl_3$ and Fe_3Al in CBPLD is consistent with the equilibrium phase diagram taking into account the difference in the measured average compositions. Also, the disappearance of Fe_3Al and $FeAl_3$ after annealing of the CBPLD sample at temperatures of about 330 and 650°C is reasonable from the point of view of the phase diagram since those are the phases most distant from the average composition.

Reaction of Fe–Al film and Si substrate started at a temperature of about 800°C with formation of $FeSi_2$ (*P4/*

[1] Sometimes this phase is denoted as FeAlSi or α-FeAlSi [8,23] or is represented according to composition as $Fe(Al, Si)_{4+\delta}$, $\delta=0.2$ (or $FeAl_4$ stabilised by Si impurity) [8,23].

[2] A compound with similar parameters $a=0.609$ nm and $c=0.944$ nm of the tetragonal unit cell is denoted as δ-$FeAl_9Si_3$ in the powder diffraction files-2 database [25] (card 20–33). Phase with tetragonal unit cell parameters $a=0.616$ nm and $c=0.949$ nm has the composition $FeAl_2Si$ according to [8].

[3] Bravais cell is primitive. Space group is not determined.

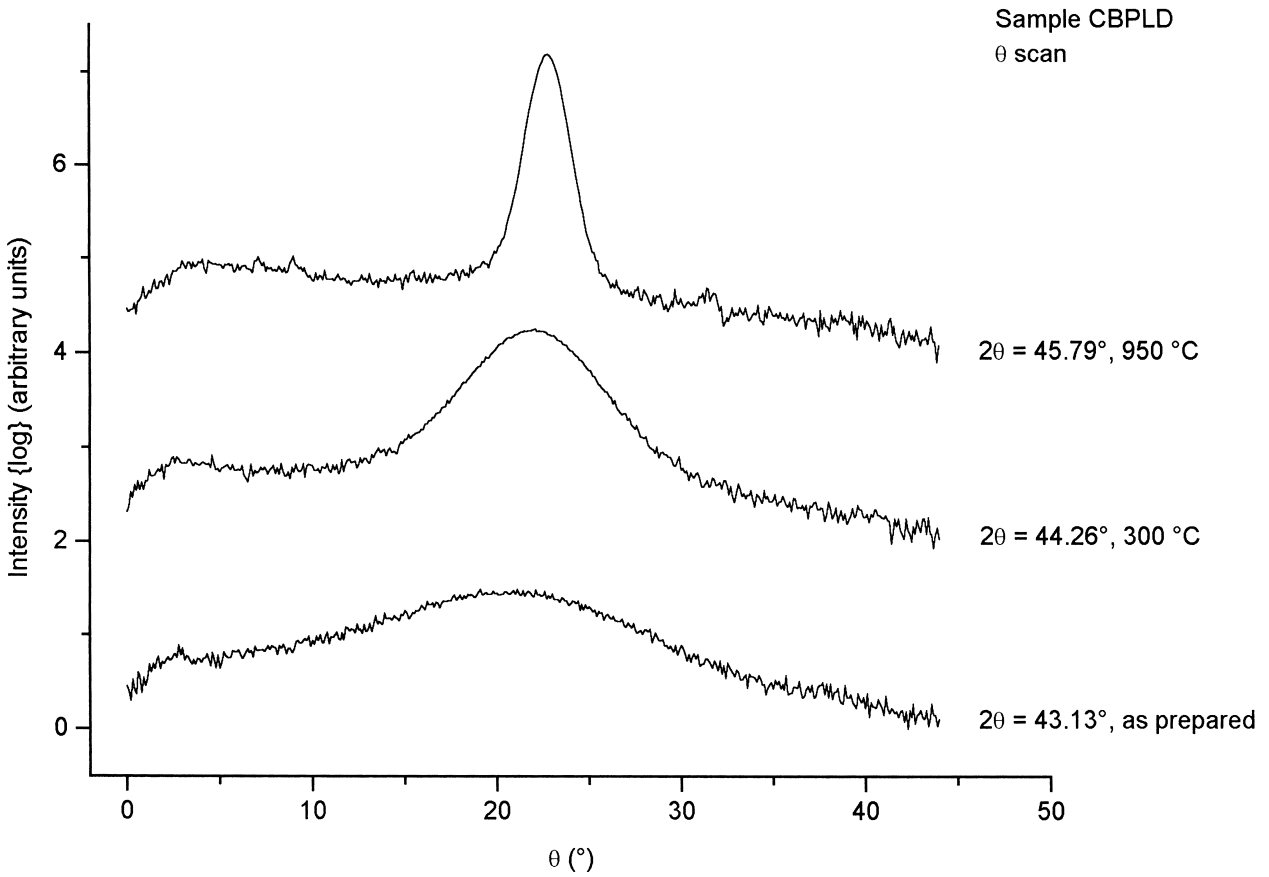

Fig. 7. Wide angle X-ray rocking curves (θ scan) for selected reflections of the CBPLD sample after different stages of annealing (reflections 110 Fe and/or 110 (Fe, Al)$_{\text{solid solution}}$ for as-prepared multilayer, 110 FeAl and/or 220 Fe_3Al for sample annealed at about 300°C and −251 γ-$FeAl_3Si$ and/or 3 0 11 Fe_2Al_8Si for sample after final annealing at 950°C). Curves were shifted to facilitate inspection. Fixed central detector positions 2θ are indicated.

mmm, $a = 0.2965$ nm, $c = 0.5090$ nm [8]) and Fe_2Al_8Si. Similarly to the CBPLD sample, the DPLD specimen changes its colour from mat-steel shade to mat dark-yellow reflecting probably the formation of the silicides.

Rocking curves of the CBPLD sample for different annealing temperatures are shown in Fig. 7. The FWHM of peaks observed decreased from 11° for the as-prepared multilayer to 5° and 1° for the sample after annealing at temperatures of about 300 and 950°C, respectively. Rocking curves recorded for other non-substrate reflections are characterised by approximately the same values of FWHM. The corresponding parameters for DPLD multilayer were 10–15° for the as-prepared sample and 2–3° after final annealing. Decrease of FWHM with increasing annealing temperature reflects the development of texture.

4. Summary and conclusions

1. Pronounced interdiffusion of Fe and Al started preferably at Fe-on-Al interfaces already at rather low temperatures (110–140°C). FeAl was formed at that temperature in the CBPLD sample only.
2. While Al-rich layers deposited by CBPLD or DPLD were X-ray amorphous, Fe-rich layers were found crystalline. Al-rich layers dissolved first at temperatures of annealing of about 140–200°C depending on thickness of the layers.
3. Full intermixing of the multilayer material occurred at a temperature, which is lower for DPLD (250°C) than for CBPLD (300°C) samples. At this temperature the formation of intermetallic compounds other than FeAl set in.
4. Intermetallic phases formed in CBPLD and DPLD samples differ. Final compounds corresponded to known equilibrium phases. Whereas FeAl and $FeAl_2$ could be detected in CBPLD in the entire temperature range of full intermixing and the $FeAl_3$ phase disappeared at 650°C and an iron-rich Fe_3Al phase formed and disappeared in a limited temperature range around 300°C, in the DPLD sample $FeAl_2$ and $FeAl_3$ were found.
5. CBPLD and DPLD samples behaved similarly with respect to reaction with substrate Si atoms. Binary intermetallic phases disappear at the beginning of this stage and silicides do form. This is where differences of CBPLD and DPLD specimens have been detected: Fe_2Al_8Si, γ-$FeAl_3Si$ and $FeAl_3Si_2$ in CBPLD and

$FeSi_2$ (tetragonal form) and Fe_2Al_8Si in DPLD. Reaction products between multilayer and Si substrate appeared at 800–825°C.

6. DPLD and CBPLD Fe–Al multilayers exhibited different reaction kinetics, which is probably due to differences in the interface composition of the as-deposited samples. Generally, the intermetallics formed in the DPLD sample correspond to an average Al content, which is considerably larger than that of the CBPLD sample.
7. During thermal treatment of both CBPLD and DPLD samples a texture is developed.

Acknowledgements

Financial support by the Deutsche Forschungsgemeinschaft (SFB 422) and by the Fonds der Chemischen Industrie is gratefully acknowledged.

References

[1] M. Shiga, T. Kikawa, K. Sumiyama, Y. Nakamura, J. Mag. Soc. Jap. 9 (1985) 187.
[2] A.W. Chowdhury, A.E. Freitag, J. Appl. Phys. 79 (1996) 6303.
[3] F. Pan, B.X. Lin, K. Rao, Phys. Stat. Sol. (a) 151 (1998) 407.
[4] L.V. Nomerovannaya, G.A. Bolotin, M.M. Kirillova, O.N. Kiseleva, L.D. Lobov, V.M. Maevskii, F.A. Pudonin, Phys. Metals Metallogr. 85 (1998) 433.
[5] O. Lenoble, Ph. Bauer, J.F. Bobo, H. Fisher, M.F. Ravet, M. Piecuch, J. Phys.: Condens. Matter 6 (1994) 3337.
[6] S. Deevi, V. Sikka, Intermetallics 4 (1996) 357.
[7] T.B. Massalski (Ed.), Binary Alloy Phase Diagrams, Vol. 1, ASM International, 1990.
[8] O. Villars, L.D. Calvert, Pearson's Handbook of Crystallographic Data For Intermetallic Phases, American Society for Metals, Metal Park, OH, 1991.
[9] T. Geilman, J. Chevallier, M. Fanciulli, G. Weyer, V. Nevolin, A. Zenkevitch, Appl. Surface Sci. 109–110 (1997) 570.
[10] C.J. Gutierrez, R. Selestrino, R.A. Mayanovic, G.A. Prinz, J. Appl. Phys. 81 (1997) 5352.
[11] J. Noetzel, K. Brand, H. Geisler, A. Gorbunov, A. Tselev, E. Wieser, W. Möller, Appl. Phys. A68 (1999) 497.
[12] J. Noetzel, H. Geisler, A. Gorbunov, R. Dietsch, H. Mai, A. Mensch, W. Möller, W. Pompe, H. Renther, A. Tselev, E. Wieser, H.H. Worch, Mater Sci. Forum 287–288 (1998) 455.
[13] H. Geisler, A. Mensch, A. Gorbunov, A. Tselev, J. Noetzel, K. Brand, H. Worch, Z. Metallkunde 90 (1999) 691.
[14] D.C. Meyer, P. Gawlitza, K. Richter, P. Paufler, J. Phys. D: Appl. Phys. 32 (1999) 3135.
[15] D.C. Meyer, K. Richter, P. Paufler, P. Gawlitza, T. Holz, J. Appl. Phys. 87 (2000) 7218.
[16] A. Tselev, A. Gorbunov, W. Pompe, Appl. Surface Sci. 138–139 (1999) 12.
[17] D. Chrisey, G. Hubler, Pulsed Laser Deposition of Thin Films, Wiley, New York, 1994.
[18] A. Shyam, S. Suwas, S. Bhargava, Praktische Metallogr. 34 (1997) 264.
[19] A.A. Levin, D.C. Meyer, P. Paufler, J. Alloys Comp. 297 (2000) 59.
[20] A.A. Gorbunov, W. Pompe, A. Sewing, S.V. Gaponov, A.D. Akhsakhalyan, I.G. Zabrodin, I.A. Kaskov, E.B. Klyenkov, A.P. Morozov, N.N. Salachenko, R. Dietsch, H. Mai, S. Völmar, Appl. Surface Sci. 96–98 (1996) 649.
[21] L.G. Parrat, Phys. Rev. 95 (1954) 359.
[22] A.A. Levin, D.C. Meyer, A. Gorbunov, A. Tselev, P. Gawlitza, H. Mai, W. Pompe, P. Paufler, Thin Solid Films, 2001, in press.
[23] R.N. Corby, P.J. Black, Acta Cryst. B33 (1977) 3468.
[24] A. Griger, Powder Diffraction 2 (1987) 31.
[25] Powder Diffraction File-2, ICDD, 1996.
[26] J. Munson, J. Inst. Met. 95 (1967) 217.